Title:	**FIREBALL DYNAMICS, ENERGETICS, ABLATION, LUMINOSITY AND FRAGMENTATION MODELING**
Author(s):	D. O. ReVelle
Submitted to:	
	http://lib-www.lanl.gov/cgi-bin/getfile?00796986.pdf

FIREBALL DYNAMICS, ENERGETICS, ABLATION, LUMINOSITY AND FRAGMENTATION MODELING

D. O. ReVelle

Los Alamos National Laboratory, P.O. Box 1663, MS J577, Earth and Environmental Sciences Division,
Atmospheric and Climate Sciences Group, Los Alamos, New Mexico 87545 USA
Email: revelle@lanl.gov

ABSTRACT

We have modeled large bolide passage through the Earth's atmosphere including the effects of dynamics, energetics, ablation, luminosity and fragmentation, including bolide porosity. In this brief paper we outline the physical processes involved in only a schematic manner. Bolide luminosity was assumed to be proportional to the time rate of change of the kinetic energy. Recently, the proportionality factor (which varies with mass, height and velocity), a semi-empirical differential luminous efficiency, has been produced in [18, 20] using the Lost City meteorite fall as a calibration event. Two schemes of fragmentation have been devised for the prediction of bolide luminosity. In the first scheme, fragmented particles are deposited into the wake after triggering by the stagnation pressure exceeding the bolide strength and these particles remain in the wake. In the second scheme, the fragmented particles are drawn forward collectively to produce an enhanced frontal area as time progresses. Considerable success was found in modeling the light curve of the Benesov bolide . The full paper with all relevant details and many additional cases will be submitted shortly to Icarus for formal publication.

1. INTRODUCTION AND OVERVIEW:

We have developed a theoretical model of bolide dynamics, energetics, ablation, luminosity and fragmentation for use in comparisons between observational material from ground-based camera and other bolide detection techniques (satellite, infrasound, etc.). This model can compute the dynamic possibilities for velocity and deceleration for either an isothermal atmosphere with either a single mean (constant) ablation parameter or a height variable ablation parameter. It can also compute the same quantities for a perfectly stratified hydrostatic, non-isothermal atmosphere as well (see below).

The energetics approach discussed further in [13] is fundamentally equivalent to the basic expression for the bolide height as a function of the entry velocity, ablation parameter, mass to area ratio, entry angle, etc. with the additional prediction of the computed velocity at which the dark flight regime begins [7]. This is accomplished by obtaining the solution of a transcendental equation relating the change of the bolide kinetic energy versus time combined with the simple ablation theory expression for the mass loss expected for a single body during entry using a single mean (constant) ablation parameter. This is probably the weakest link of all predicted parameters in the model, yet it is only used to predict the velocity at which ablation ceases as a function of the D parameter of ReVelle. Typical D values utilized were assumed to range from 2.303 to 4.605 (90 - 99 % kinetic energy removed at the end height) . The latter D value was calibrated through a detailed analysis of the photographic data of the Lost City, Innisfree and Pribram meteorite falls [11].

The ablation model is basically the one developed originally in [9] which predicts the prevailing stagnation point ablation mechanism somewhere between the limits of vaporization and melting as a function of the dimensionless ablation interaction parameter, k ($= V_\infty^2 /2Q_{vap}$), where V_∞ = pre-atmospheric, initial meteoroid velocity and Q_{vap} = energy of ablation per unit mass for ablation of one of at least five possible, distinct meteoroid groups). The model includes almost all previously identified forms of heat transfer with the exception of so-called precursor ionization effects, i.e., free stream absorption which occurs well ahead of the bolide and interference heating effects, i.e., viscous boundary layer-strong shock wave interactions at progressively higher altitudes, but at transitional Kn number~ 1). Absorption of the radiative shock wave flux is not included in the

calculations due to a very large uncertainty in both the precise mix of constituents in the parent meteoroid and in their radiative properties at high temperatures (with multiply ionized states, etc.). Rotation and lift (non-ballistic forces) have not been included in the analysis. Two groups [2, 8] have recently considered rotation effects regarding significant flickering of light curves that has been observed on occasion. The former group [2] concluded that rotation was not a significant factor in altering meteoroid ablation processes (at least for the fall of the Innisfree meteorites) for a rather unusual proposed meteoroid shape, even though under certain conditions rotation could be expected to influence pulsations observed on fireball light curves (significant changes in stellar magnitude which would translate to extremely significant changes in the predicted light intensity).

Theoretical non-dimensional heat transfer expressions are computed for either laminar or turbulent convective/conductive heat transfer through the gas cap as well as for radiative emission from the strong shock front in the absence of ablation products absorption effects. These calculations also neglect the so-called precursor ionization phenomena (free stream absorption effect). These are discussed further in [13]. Furthermore, we have continuously computed all of the relevant parameters as a continuous function of the Knudsen number, Kn, for all of the extremes from free molecular flow (Kn >> 1) to continuum flow (Kn << 1).

Shape change during entry is accomplished using the shape change parameter, μ, which has been measured directly in [19] for a number of very precisely measured bolides. Most cases had $0 < \mu < 1$, but about 1/3 of the cases had $\mu < 0$ and for all cases μ was usually a function of height (or equivalently time). The former regime encompasses the classical self-similar, no shape change result ($\mu \equiv 2/3$). The latter limit ($\mu < 0$) includes the so-called catastrophic "pancake" fragmentation regime that was rediscovered by Zahnle, Chyba and Thomas, by Hills and Goda, etc. during the predictions of the impact of Comet Shoemaker-Levy-9 into Jupiter's atmosphere. The regimes of flight corresponding to different constant μ values along the trajectory were summarized in [16, 17, 19]. We have not yet devised a theoretical procedure to deal with changes of μ during entry despite the fact that observations clearly show that $\mu = \mu(z)$.

The luminosity prediction is based upon the fundamental premise that the light emitted in a specific electromagnetic pass-band is proportional to the time rate of change of the kinetic energy of the bolide. In order to complete the prediction currently, a semi-empirical luminous efficiency parameter has been utilized from [18, 20] as a function of mass, air density and velocity. This function has been computed only for the panchromatic pass-band of the photographic emulsion used to detect these bright bolides. Since we have now computed the equilibrium temperatures surrounding the bolide as well, we can in principle correct the prediction for any other pass-band of interest.

Fragmentation is calculated in two limiting extremes currently. Once triggered by the stagnation pressure exceeding the strength of the bolide (as modified by cracks, porosity, etc.), the fragmented particles are either transferred to the wake and remain there or are allowed after a specified time lag to be drawn forward toward the main leading fragment. The bolide luminosity is now being calculated for either of these two respective limiting conditions.

Porosity is explicitly included in the model formulation and as shown in [17], can significantly effect the luminosity prediction.

2. MODERN BOLIDE FRAGMENTATION MODELING APPROACHES: RELAXATION OF THE SINGLE-BODY THEORY LIMITS

There are several possible types of fragmentation processes, but only two fundamental triggering mechanisms have been proposed in the recent literature. These mechanisms include both a thermal and a mechanical initiation process, but severe temporal limitations of the thermal mechanism argue against its general applicability, except perhaps for meteoroids with very high thermal conductivity, such as nickel-iron meteorites. This is because the time needed to produce fragmentation by thermal effects is far too long compared to the available entry flight time.

Among the mechanism proposed starting about 1970 and beyond, we have:

i) An enhanced frontal area with the air drag increasing as the conventional drag of a single-body times the number of fragments produced during break-up to the 1/3 power [1]. Unfortunately, this model produced very unreliable

entry results when compared against very precise observations.

ii) Heat transfer area >> Air drag area: This can be due to porosity effects [12] for example even without fragmentation occurring, but other researchers have also predicted this behavior for very different reasons.

iii) Quasi-continuous fragmentation of small particles: Unlike the other processes mentioned here this process can be adequately described using the simple ablation theory formulation. It is mentioned here for completeness only.

iv) Progressive fragmentation or cascade break-up processes [3]. This progressive cascade process is the one utilized in this paper. Its primary advantage is that once fragmentation begins there is no further need to specify any other parameters to describe the process.

v) Catastrophic, "pancake type" break-up: This is presumed to occur [16] for the very largest bolide sizes since the lateral pressures surrounding such bolides are much smaller than the forward pressures at the strong shock front which can lead to large and rapid, lateral spreading. The μ parameter, initially introduced originally by Levin, incorporated this possibility as well if $\mu < 0$ [16].

This latter approach has been recently and actively pursued by a number of authors for the modeling of the entry of Comet Shoemaker-Levy 9 into the atmosphere of Jupiter.

Recently in [16] the concept of the fragmentation scale height was introduced which is defined by the vertical distance over which the frontal cross-sectional area increases by 1/e as the bolide descends deeper into the atmosphere. It was shown in [16, 17] that for most large bolides, $\mu > 0$ and that the <u>single-body</u> limit:

i) $|H_p / H_f| \ll 1$

is normally maintained, whereas if:

ii) $H_p/H_f \gg 1$

where

$H_p = -p/\{\partial p/\partial z\}$ = pressure scale height
$H_p = RT/g$, if isothermal and hydrostatic
$H_f = -f/\{\partial f/\partial z\}$ = fragmentation scale height
$f \equiv A(z)/A_\infty$
$A(z)$ = instantaneous meteor frontal area
A_∞ = initial meteor frontal area

If the latter limit is correct, then the dynamics is described by equations that fully include the dominance of various types of fragmentation effects. In our current modeling we are able to compute two fragmentation limits, i.e., rapid wake transfer of fragments subsequently with either collective or non-collective wake behavior. These limits are illustrated below when comparisons are made against observations.

3. THEORETICAL MODELING APPROACHES: RECENT LOS ALAMOS MODELING EFFORTS

3.1 <u>Bolide Groups and Porosity</u>

Given the inputs of the bolide initial entry velocity, horizontal entry angle, initial radius, initial shape, shape change parameter, μ, (assumed to be a constant), bulk density (or equivalently the uniform volume porosity), etc. we can completely predict for all possible flow regimes (from free molecular to continuum flow), numerous aspects of the entry process including detailed thermal equilibrium temperature effects and infrasound production rates, etc. Some modeling exceptions include aerosol production, Earth-impact cratering efficiency (or Tsunami production in the ocean), flow chemistry and associated electromagnetic effects, etc. We have utilized the D parameter, energetics approach in [13]. This approach has been a recent modification of the physical basis presented in [9-14, 16-17] and includes both a constant as well as a variable ablation parameter, σ, a variable temperature atmosphere (non-isothermal conditions as a function of season with both the pressure and density scale height functions of altitude and season, etc.). The model in totality is a progressive improvement of theoretical models developed by numerous earlier workers. It is fundamentally based on a number of studies by Ceplecha and McCrosky, by Sekanina and by Wetherill and ReVelle that have ascertained that there are at least five discrete bolide groups entering the Earth's atmosphere whose properties transcend the range

of sizes from ordinary small camera meteors to large bolides [7]. We show below the group version developed in [12, 17] that includes porosity, but a version that was accomplished using a uniform bulk density bolide model is also extremely similar [17].

First we examined both uni-axial tensile and compressive strength data from samples tested in the laboratory (taken largely from the numerous measurements in [1]). Both types of strengths seem to have a role to play in the fragmentation process since clearly lateral displacements are related to tensile strengths whereas compressive strength are more important relative to imposed frontal pressures at the stagnation point. For a rotating, irregularly shaped body it is not clear which of these should be the dominant strength to consider so we have combined them together somewhat interchangeably for now. The laboratory samples tested included Nickel-iron meteorites, ordinary and carbonaceous chondritic materials as well as very porous substances. In Figures 1 and 2 we display the resulting curve fits of these quantities that we have used in our model for specifying the onset of fragmentation.

In Figure 1, we have plotted the graphical fit of the meteoroid bulk density in kg/m^3 versus the compressive strength of the samples tested in Pa (1 bar = 10^5 Pa). The curve fit can clearly be seen to be a highly correlated function. Even so the difference between the curve-fitted values and the individual data points can be very significant in terms of predicting the altitude where break-up will occur. For the specific case of 2.0 kg/m^3 (carbonaceous chondrite) the difference between the curve fitted compressive strength value and the actual measured value is very significant. The predicted break-up height difference is a function of velocity, etc., but can differ by several km for this situation. Thus, even if we knew the breaking strength exactly (if there were no cracks from space collisions, etc.), we would still have a significant uncertainty in the exact break-up height depending on whether we utilize a continuous curve-fitted functional relationship or specific laboratory measurements. A similar situation is also found at very low porosities (~0-10 %) when comparing compressive strengths against uniform volume porosity curve- fitted values against the individually measured values.
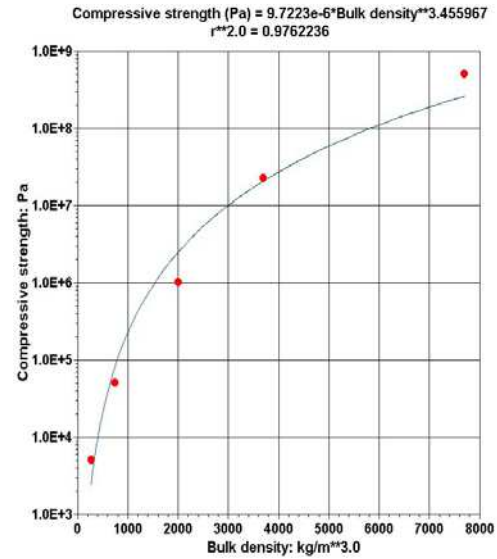

Figure1: Meteoroid bulk density (kg/m^3) versus compressive strength (Pa).

In Figure 2 we have plotted the compressive or tensile strength versus the porosity of the body. Again very high cross-correlations have been found between these two parameters.
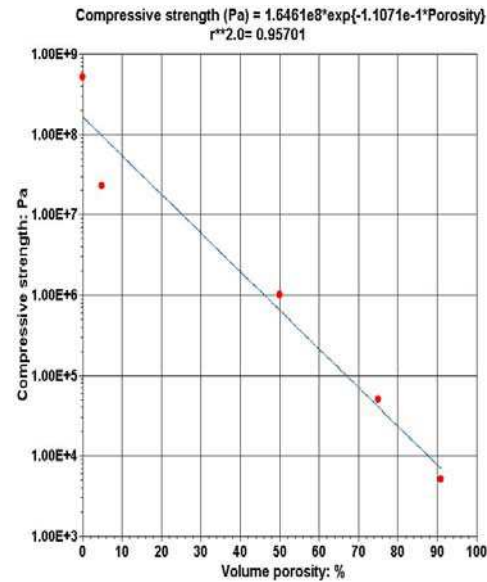

Figure 2: Uniform meteoroid volume porosity (%) versus compressive strength (Pa).

In Figure 3, we display the bolide bulk density for uniformly porous bodies as a function of the height averaged ablation parameter (mean) for each bolide group. The designations: 0, I, II, IIIA and IIIB are for small irons (< $2.0 \cdot 10^5$ kg), ordinary chondrites, carbonaceous chondrites, strong cometary material and weak cometary

material respectively. Within the boundaries of the plot the compressive strengths of the corresponding bolides are contoured. Actual triggering of break-up was allowed when stagnation pressures exceeded a value only 1/5 as large as in the plot to allow for cracks due to space collisions, non-uniform porosity, etc.
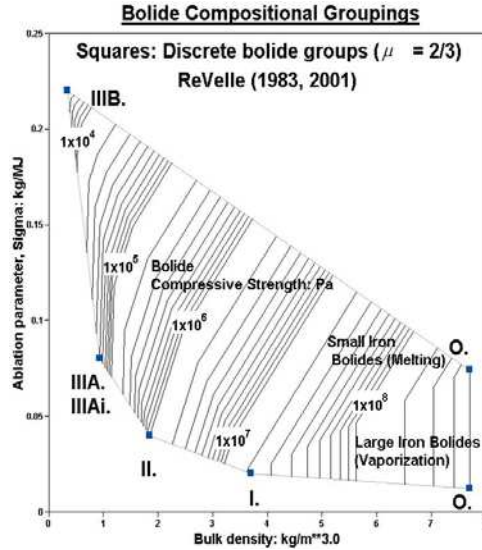

Figure 3: Meteoroid bulk density (kg/m^3) versus bolide ablation parameter (s^2/km^2) as a function of the compressive strength (Pa) for the five fundamental fireball groups.

For any specific group or any measured bulk density of recovered meteorites, we can predict numerous features of the entry given the specific properties identified for each bolide type.

As a result of our modeling approach we can now identify several different regimes of behavior. The only significant change found compared to the results determined in [16] is the presence of a fragmentation regime with a generally small positive fragmentation scale height with either collective wake behavior after rapid wake transfer or non-collective wake behavior. This regime is possible for $2/3 < \mu < 0$.

3.2 Fragmentation Modeling Approach

We have determined an additional solution to the fragmentation dynamics not discussed in Kiruna [16]. This solution corresponds to the case of fragmentation with rapid wake transfer followed shortly by a collective wake behavior such that the fragments are drawn forward toward the leading piece (assumed to be present) with a progressive enhancement of the frontal

area. The number of fragments produced is currently left as an unspecified free parameter of the problem, but efforts are also underway to define the limiting number of fragments as a function of the bolide group, radius, bulk density, porosity, etc. Since the fragmentation process is most likely non-unique, it is unlikely that there is a single solution possible just as in the case of turbulence modeling theories. We have continued, in the absence of specific wake dynamics solutions, to only model fragmentation and the light emission process in two distinct limits which begin with rapid wake transfer of fragmented particles that continue to break as time proceeds, followed by:

    i)   Non-collective wake behavior
    ii)   Collective wake behavior

In the former case i) all particles in the near-wake remain in the wake whereas in ii) the particles are all drawn forward producing an enhanced frontal area of fragmented particles with a small positive fragmentation scale height. In case i) the fragmentation scale height is < 0 as it is for the single body limit given earlier above. As the particles are transferred into the wake they do not respond instantaneously to produce light, so we have arbitrarily inserted a time lag that is a function of the speed of the body and its degree of ablation, etc. This time lag varies from a few tenths of a second at lower entry velocities from 11-15 km to $< 10^{-3}$ s at progressively higher entry speeds. In the former limit (non-collective wake behavior), the instantaneous values at any height of the radius, frontal cross-sectional area, mass and mass/area ratio are changed in a very different manner than they are for collective wake behavior. These extreme changes greatly influence the luminosity prediction.

4. FUNDAMENTAL EQUATIONS OF BOLIDE ENERGETICS (D PARAMETER)

Kinetic energy changes due to ablation (β) and air drag (α) from simple ablation theory in [11]:
$$E_k(z) = E_{k\infty} \cdot \exp[-D]$$

where

$$E_k = (1/2) \cdot m \cdot V^2; \quad D = \alpha + \beta$$

α = Kinetic energy decay due to air drag
β = Kinetic energy decay due to ablation D = 4.605 (2.303) for 99 % (90 %) E_k depletion

$$V(z) = V_\infty \cdot \exp[(\sigma/4)\cdot\{V_\infty^2 - V^2(z)\}]\cdot\exp[-D/2]$$

where

E_k = instantaneous bolide kinetic energy
m = instantaneous meteor mass
V = instantaneous meteor velocity
σ = instantaneous ablation parameter

End height calculation [14]:

$$z_{KE}(V) = -H_p\cdot\{\ln(p_\infty^*/p_o)\cdot\exp[-\Phi\cdot V_\infty^2]\cdot[D-D']+\exp[-z'/H_p]\}$$

$$D' = -\{Ei[\Phi\cdot V_\infty^2]- Ei[(\Phi\cdot V^2(z)] -\ln(V_\infty/V(z))^2-[(\sigma/2)(V_\infty^2-V^2(z))]\}$$

$$z' = -H_p\cdot\{\ln(p_\infty^*/p_o)\cdot(2g\cdot H_p/V_\infty^2)\}; \quad \Phi \equiv \sigma\cdot(1-\mu)/2$$

where

z = geopotential height (km)
z' = height where the drag force first balances the weight component along the trajectory
p_∞^* = modified ballistic entry parameter (for $\theta \geq 10$ deg (plane parallel atmosphere)`
p_o = surface atmospheric pressure (Pa)
g = acceleration due to gravity
θ = horizontal entry angle (deg)

In addition, we use three additional heights that have been derived in order to produce the height maximized quantities of $m\,V\cdot dV/dt$, $m\cdot dV/dt$ and dV/dt in order to evaluate key regimes as a function of the ablation parameter, σ and the shape change parameter, μ, etc.:

$$z_i(mVdV/dt:Max)=-H_p\cdot\ln\{(p^\bullet(z)/p_o)/[1.5+(\sigma\mu/2)\cdot V^2(z_i)]\}$$

$$z_{ii}(mdV/dt:Max)=-H_p\cdot\ln\{(p^\bullet(z)/p_o)/[1+(\sigma\mu/2)\cdot V^2(z_{ii})]\}$$

$$z_{iii}(dV/dt:Max)=-H_p\cdot\ln\{(p^\bullet(z)/p_o)/\{1+(\sigma(\mu-1)/2)\cdot V^2(z_{iii})\}]$$

5. THEORETICAL LUMINOSITY SOLUTION PROCEDURES

Observations of the spectra from bolide light emission indicate the dominant role played by meteor atoms and ions (emission lines) with Nickel-iron usually assuming a dominant role in many meteor spectra. For this reason we have followed the classical meteor assumption that the total light output is proportional to the time rate of change of the kinetic energy of the bolide as in [11] and summed over all fragments. The proportionality constant is the differential luminous efficiency that has recently been reinvestigated in [18, 20]. Our semi-empirical differential luminous efficiency parameter was completely calibrated using the very well observed entry of the Lost City meteorite fall (January 3, 1970) during the era of the US Prairie Network. Using this engineering type approach, we have calculated the light emission with respect to a panchromatic pass-band. The resulting equation is given by [17]:

$$I_L = -\tau_L\, dE_k/dt$$

where

I_L = instantaneous light emission: watts/steradian
τ_L = differential luminous efficiency
dE_k/dt = instantaneous time rate of change of the kinetic energy of the bolide

$$dE_k/dt = \Sigma\,\{m(z)\cdot V(z)\cdot dV/dt \cdot[1+\Delta(z)]\}$$

or, equivalently:

$$dE_k/dt = -\Sigma\,\{-0.50\cdot Ro^2(z)\cdot p(z)\cdot V(z)\cdot[1+\Delta(z)]\}$$

where

$\Delta(z) = 2.0/\{\sigma(z)\cdot V(z)^2\}$
dV/dt = instantaneous meteor deceleration
$p(z)$ = ambient pressure along the trajectory
$R_o(z)$ = instantaneous line source blast wave relaxation radius [15]
$R_o = M(z)\cdot d(z)$; for a single-body model
$R_o \equiv \{[\rho(z)\cdot V(z)^2\cdot C_D\cdot A(z)]/p(z)\}^{1/2}$ in general, including fragmentation
$M(z)$ = Mach number of the bolide
$d(z)$ = instantaneous bolide diameter
C_D = drag coefficient (= $C_D\,(S_f, Kn)$)
S_f = shape factor (= 1.208 for a sphere)

In [17] it has already been shown that the predicted light for a porous body exceeds that for a nonporous body under otherwise identical conditions. This is important because it allows an additional free parameter to be used in modeling the observational data, a parameter that seems to be physically meaningful for many of the bolide observations. The additional importance of this parameter is that as the porosity disappears the two model approaches become identical.

In addition to light predictions in watts $\cdot$steradian^{-1} or in stellar magnitude units, we have also calculated the equilibrium, chemically reacting, air temperatures both in the strong

shock region as well as across the gas cap boundary layer. We have also scaled these temperatures appropriately in the wake in terms of earlier numerical predictions from line source blast wave theory due to Plooster. This is important since the conversion from watts/steradian to stellar magnitude requires a wake temperature evaluation. From direct spectroscopic measurements these temperatures have been determined to be about 4500 deg K ("warm" component) and 10,000 deg K ("hot" component) respectively [7]. In addition, we are also investigating both non-equilibrium temperatures and the case of frozen flow conditions, i.e., the opposite extreme of equilibrium, chemically reacting flows.

6. PREDICTIVE MODELING: COMPARISONS AGAINST OBSERVATIONAL DATA

In this brief version of the full paper that will be submitted to Icarus, we will only include a few preliminary predictions in order to illustrate the type of results that the new model is capable of generating.

In Figure 4, we plotted the light emission in watts/steradian versus time for the Bensov bolide (May 7, 1991) using 15 % uniform volume porosity for the case of collective wake behavior, with D = 4.605 for all cases (99% E_k depletion). It is clear that the predicted fragmentation event produced a major influence on the light curve.

Figures 4-6 (for the Benesov bolide entry for a total of either 8 or 16 fragments as indicated) illustrate respectively, the light curve versus time for collective wake behavior, stellar magnitude versus height for collective wake behavior and stellar magnitude versus height for non-collective wake behavior. Finally in Figure 7, "pancake" behavior for $\mu = -0.50$ = constant is illustrated. Benesov data are from Borovicka and Spurny, (personal communication, 2001) for EN070591. It is clear from Figure 7, as expected in [16, 19], that "pancake" behavior will not explain the observed Benesov light curve. We have also plotted in Figure 8, the predicted line source blast wave radius (R_o) versus height for Benesov, using a US Standard atmosphere for middle latitude summer conditions with collective fragment behavior in the wake.

In addition, in Figures 9-11, we have also plotted contour plots for the line source blast wave radius versus time versus the luminosity in watts/steradian, for the line source blast wave

radius versus time with luminosity in stellar magnitude and for the line source blast wave radius versus time versus the equilibrium air temperature in deg K (at the strong shock stagnation point). For these last three plots, entry conditions were assumed identical to those for Benesov given earlier with the exception that the entry velocity was reduced to 14.18 km/s (approximately the value for the Lost City meteorite fall in 1970).

As a final topic in Figure 12, we have plotted the computed dimensionless integral acoustic efficiency for Benesov versus height [5, 6, 11]. We define the acoustic efficiency as the quasi-linear pressure wave kinetic energy density at x = 1 (one blast wave radius away from the entry trajectory) compared to the bolide kinetic energy density at any height along the trajectory. During the "flare", i.e., for the gross-fragmentation event near 23 km, or ~25 km for the summer non-isothermal, US Standard atmosphere, the acoustic efficiency decreases to ~ 0.3 %, just as the luminosity is predicted to increase. This is important since we are trying to account for all of the bolide energy changes in a temporal power balance statement. Predicted integral acoustic efficiencies range from ~10^{-3}- 2 %
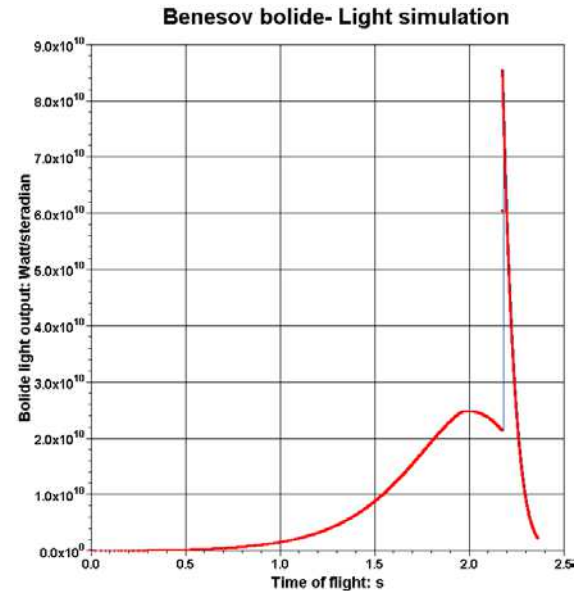

Figure 4: Bolide luminosity (Watts/steradian) versus time of flight (s) along the observed entry trajectory for the Benesov bolide on May 7, 1991 for collective wake behavior for 8 fragments.

Benesov: May 7, 1991: 23h 03m UTC
Blue squares- Modeled light curve, Red circles- Sampled light curve
Entry parameters: Sphere-unchanging shape (for simplicity)
Rinf = 0.50 m, Zrad = 9.4 deg, Vinf = 21.18 km/s, Uniform volume porosity = 15 %,
8 fragments allowed in progressive fragmentation- Collective wake behavior
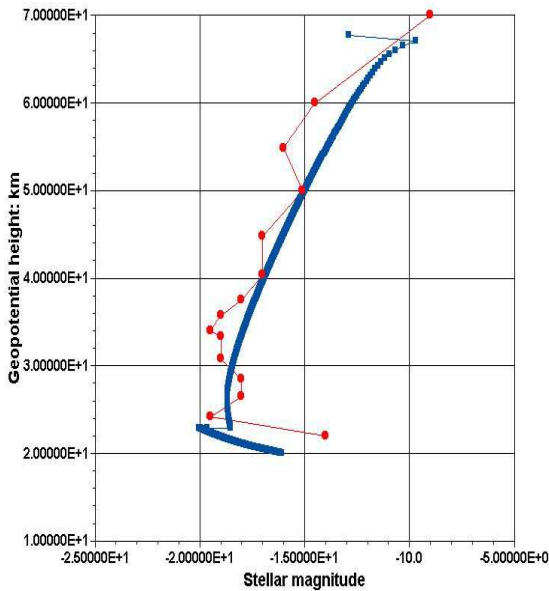Initial mass: 1647 kg, Predicted terminal mass ~59.5 kg

Figure 5: Bolide luminosity (stellar magnitude) versus height (km) for the Benesov bolide on May 7, 1991: Collective wake behavior assumed.

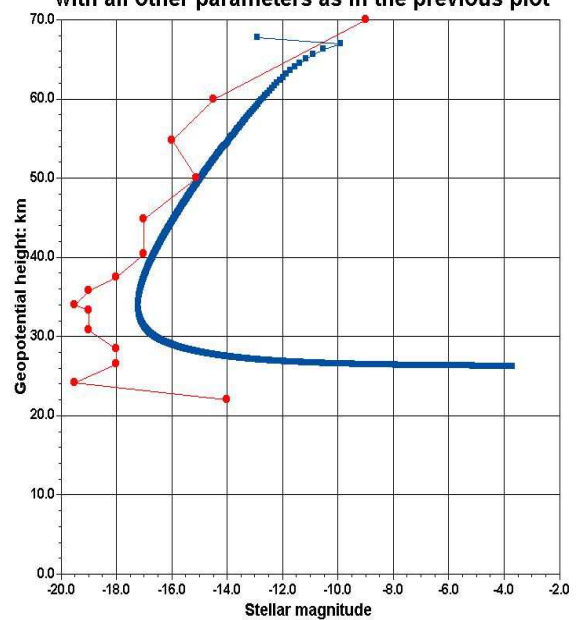Benesov: "Pancake" model results: "Mu" = - 0.50 with all other parameters as in the previous plot

Figure 7: Bolide luminosity (stellar magnitude) versus height (km) for the Benesov bolide on May 7, 1991: Catastrophic "pancake" behavior assumed (with μ = -0.50 = constant).

Benesov: "Mu" = 2/3, 15 % porosity, 16 fragments, non-collective wake behavior with all else as in the nominal collective wake behavior case.
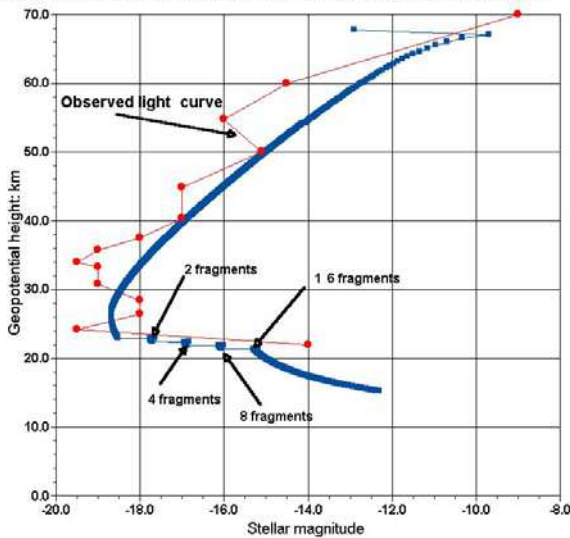

Observed light curve

2 fragments   1 6 fragments

4 fragments   8 fragments

Figure 6: Bolide luminosity (stellar magnitude) versus height (km) for the Benesov bolide on May 7, 1991: Non- collective wake behavior assumed.

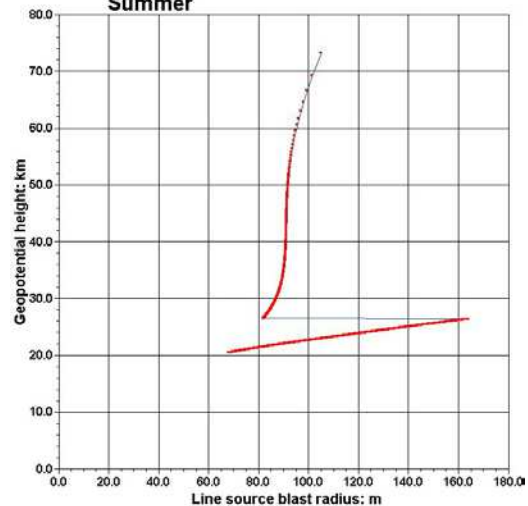Benesov test: Sigma variable Non-isothermal atmosphere- Summer

Figure 8: Line source blast wave relaxation radius (m) versus height (km) for the Benesov bolide. Collective wake behavior for 8 fragments assumed.
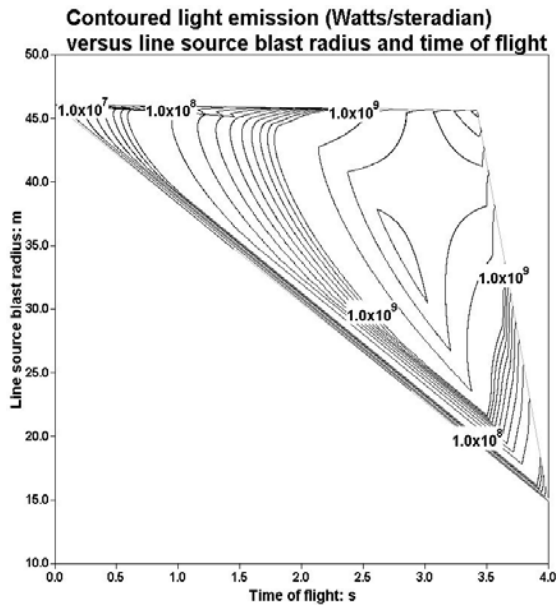
Contoured light emission (Watts/steradian) versus line source blast radius and time of flight

Figure 9: Line source blast radius (m) versus time of flight (s) for contoured values of bolide luminosity for V= 14.18 km/s with all other parameters as for the Benesov bolide above.

Strong Shock Temperature Contours ($\beta \equiv 90°$) versus Blast radius and Time of Flight
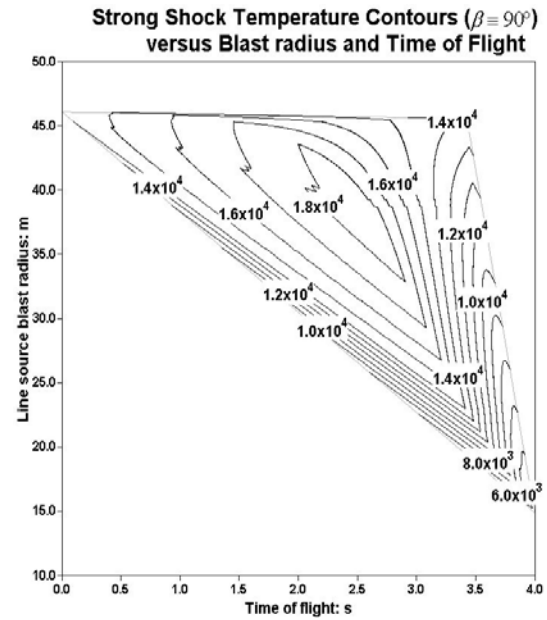

Figure 11: Line source blast radius (m) versus time of flight (s) for contoured values of the stagnation point, strong shock equilibrium air temperature, for V = 14.18 km/s with all other parameters as for the Benesov bolide above.
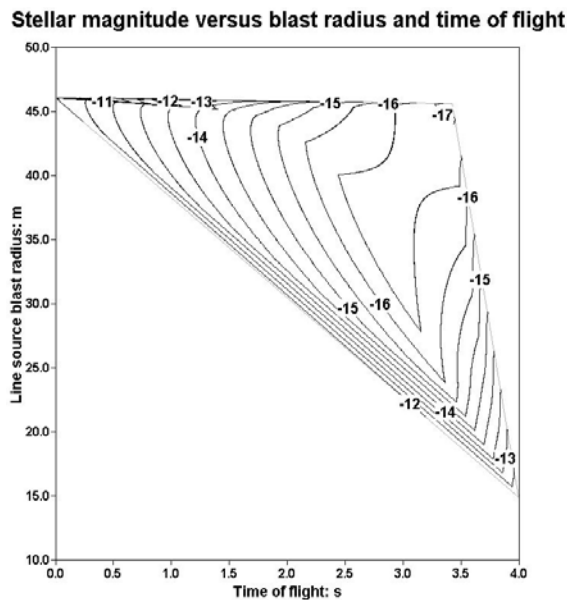
Stellar magnitude versus blast radius and time of flight

Figure 10: Line source blast radius (m) versus time of flight (s) for contoured values of stellar magnitude for V= 14.18 km/s with all other parameters as for the Benesov bolide above.
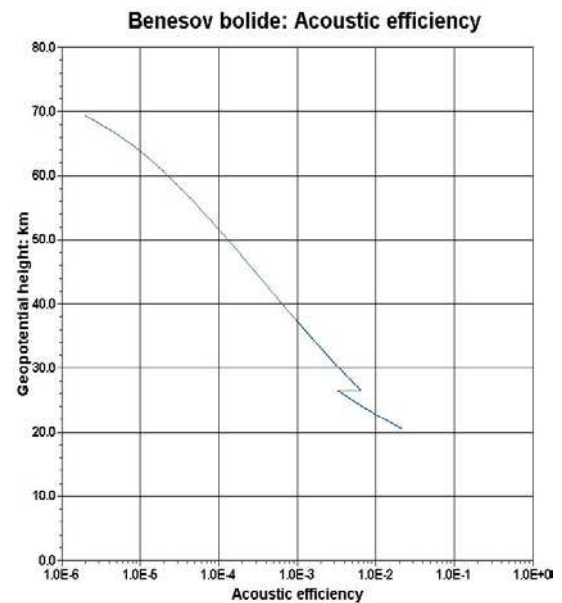
Benesov bolide: Acoustic efficiency

Figure 12: Integral , dimensionless, acoustic efficiency versus geopotential height (km) for the Benesov bolide.

7. SUMMARY AND CONCLUSIONS

We have constructed an entry model that depends on a number of earlier approaches that have all been put together for the first time. The model simultaneously includes all relevant dynamics, energetics, ablation, luminosity (for a panchromatic pass-band) and fragmentation (for two extreme dynamical limits within the wake). The combination of all of these processes for the prediction of bolide luminosity relies heavily on the semi-empirical differential luminous efficiency parameter developed in [18, 20]. We are in the process of testing our predictions on a number of new cases to verify that an essentially correct calibration has been made. In order to construct the fragmentation model, a key assumption had to be made, i.e., that there was a leading fragment during the entry that remained the leading body throughout the flight. Clear evidence from the Moravka bolide (personal communication with J. Borovicka, 2002) shows that the leading fragment changes its position during the flight. In addition, it is envisioned that for the weaker cometary bodies, there may not ever be a leading fragment at all, only a large group of very small fragments. Thus, future work must include detailed dynamical calculations of the fragmented particles within the wake. It must also include the incorporation of non-equilibrium and frozen flow wake temperatures and compute the corresponding spectrum for an assumed meteoroid composition, etc. These calculations are necessary for the proper conversion of panchromatic luminosity to stellar magnitude since the luminosity is a direct function of the wake air temperature(s) where the radiation originates.[7]

8. REFERENCES:

1. Baldwin, B, and Y. Sheaffer, J. Geophys. Res., 76, 4653-4668, 1971.
2. Beech, M., Mon. Not. Roy. Astron. Soc., 326, 937-942, 2001.
3. Bess, T.D., NASA TP 1333, 1979.
4. Brown, P.G., D.O. ReVelle and A.R. Hildebrand, Meteoroids2001-Conference Proceedings, ESA SP-495, ed. B. Warmbein Kiruna, Sweden, pp. 497-506, 2001.
5. Brown, P.G., D.O. ReVelle, E. Tagliaferri and A.R. Hildebrand, Meteoritics and Planetary Science, 37, 661-675, 2002.
6. Cox, E. F., Handbuch der Physik, vol. XLVIII, pp. 455-478, ed. J. Bartels, Springer-Verlag, Berlin, 1958.
7. Ceplecha, Z, J, Borovicka, W. Graham Elford, D.O. ReVelle, R.L. Hawkes, V. Porubcan and M. Simek, Space Science Reviews, 84, 327-471, 1998.
8. Novikov, G.G. and O.V. Sokolov, Meteoroids2001-Conference Proceedings, ESA SP- 495, ed. B.Warmbein, Kiruna, Sweden, pp. 287-294, 2001.
9. ReVelle, D.O., J. Atmos. Terr. Phys., 41, 453-473,1979.
10. ReVelle, D.O., IAU Symposium No. 90, Solid Particles in the Solar System, eds. I. Halliday and B.A. McIntosh, D. Reidel Pub. Co., Dordrecht, 185-198, 1980.
11. ReVelle, D.O., A Predictive Macroscopic Integral Radiation Efficiency Model, J. Geophys. Res., 85, 1803-1808, 1980.
12. ReVelle, D.O., Meteoritics and Planetary Sci., 18, 386, 1983.
13. ReVelle, D.O., Meteoroids 2001-Conference Proceedings, ESA SP-495, ed. B. Warmbein, Kiruna, Sweden, pp. 149-154, 2001a.
14. ReVelle, D.O., Meteoroids2001-Conference Proceedings, ESA SP-495, ed. B. Warmbein, Kiruna, Sweden, pp. 179-184, 2001b.
15. ReVelle, D.O., Meteoroids2001 Conference Proceedings, ESA SP-495, ed. B. Warmbein, Kiruna, Sweden, pp. 483-490, 2001c.
16. ReVelle, D.O, Meteoroids2001-Conference Proceedings, ESA SP-495, ed. B. Warmbein, Kiruna, Sweden, pp. 491-496, 2001d.
17. ReVelle, D.O., Meteoroids2001-Conference Proceedings, ESA SP-495, ed. B. Warmbein, Kiruna, Sweden, pp. 513-518, 2001e.
18. ReVelle, D.O. and Z. Ceplecha, Meteoroids2001-Conference Proceedings, ESA SP-495, ed. B. Warmbein, Kiruna, Sweden, pp. 507-512, 2001a.
19. ReVelle, D.O. and Z. Ceplecha, Meteoroids2001-Conference Proceedings, ESA SP-495, ed. B. Warmbein, Kiruna, Sweden, pp. 179-184, 2001b.
20. ReVelle, D.O. and Z. Ceplecha, Fragmentation Model of Meteoroid Motion and Radiation During Atmospheric Penetration, ACM2002 Conference Berlin, Germany, July 29- August 2, 2002, 2002 (This conference).